Catal Lett (2009) 127:400–405
DOI 10.1007/s10562-008-9708-x

High Activity in Catalytic Oxidation of Benzyl Alcohol with Molecular Oxygen over Carboxylic-Functionalized Carbon Nanofiber-Supported Ruthenium Catalysts

Tiandi Tang · Chengyang Yin · Ni Xiao ·
Mingyi Guo · Feng-Shou Xiao

Received: 15 February 2008 / Accepted: 26 September 2008 / Published online: 15 October 2008
© Springer Science+Business Media, LLC 2008

Abstract Carboxylic-functionalized carbon nanofiber-supported Ru catalysts were prepared from the treatment of carbon nanofiber in HNO_3–H_2SO_4 media, followed by impregnation with $RuCl_3$ solution, dryness, calcination, and reduction procedures. Interestingly, carboxylic-functionalized carbon nanofiber-supported Ru catalysts show a good performance in oxidation of benzyl alcohol with molecular oxygen. In contrast, after partial removal of carboxylic groups on the surface of carbon nanofiber-supported Ru catalysts, the activities are reduced significantly. These results suggest that the carboxylic species on carbon nanofiber-supported Ru catalysts play an important role for the promotion of catalytic activity.

Keywords Carbon nanofibers · Supported Ru catalyst · Carboxylic species · Oxidation of benzyl alcohol

1 Introduction

Carbon nanofibers (CNF) and carbon nanotubes (CNT) as catalyst supports have been widely used in light alkenes hydrogenation [1–5], α,β-unsaturated aldehydes hydrogenation [6–18], nitrobenzene hydrogenation [19–21], cyclohexene hydrogenation [22], alkene hydroformylation [6, 23], ammonia synthesis [24, 25], cyclohexanol dehydrogenation [26, 27], Fischer–Tropsch synthesis [28–31], decomposition of NO [32], *n*-hexane isomerization [33], aromatic hydrogenation [34, 35], and aniline oxidation [36, 37]. Compared with the conventional catalyst supports such as activated carbon, γ-Al_2O_3, and SiO_2, CNF, and CNT supports have obvious features such as graphitic nature and high capability of hydrogen storage, which are favorable for the metal-support interaction [2, 8–12, 32, 37], the electron transfer between support and metallic particles [2, 24, 25], and the formation of surface hydrogen atoms on the active sites [33]. Notably, CNF and CNT supported metal catalysts are mainly focused on hydrogenation [1–31, 34, 35], but there are a few examples for heterogeneous oxidation of hydrocarbons [38] because CNF and CNT are easily destroyed in oxygen atmosphere at relatively high temperature. In this work, we show an example for catalytic oxidation of benzyl alcohol with molecular oxygen at relatively low temperature (140 °C) over CNF-supported Ru catalysts. Very interestingly, these catalysts are catalytically active and the surface carboxylic species play an important role for the promotion of catalytic activity.

2 Experimental

2.1 Treatment of CNF

CNF was obtained by catalytic decomposition of methane in a stainless-steel tube reactor with Ni/Al_2O_3 as a catalyst according to reported literature [39]. The treatment of CNF was typically as follows: (1) 3.0 g of CNF were grounded into below 200 meshes, followed by addition of 32 mL of mixed concentrated nitric acid (65%) and sulfuric acid (95–98%) with a 1:1 volume ratio. (2) After treatment in a stainless-steel autoclave with teflon liner at 120 °C for 100 min with a magnetic stirrer, the sample was thoroughly washed with deionized water, filtrated at room temperature

---

T. Tang · C. Yin · N. Xiao · M. Guo · F.-S. Xiao (✉)
College of Chemistry and State Key Laboratory of Inorganic Synthesis and Preparative Chemistry, Jilin University, Changchun 130023, People's Republic of China
e-mail: fsxiao@mail.jlu.edu.cn

and dried at 110 °C for 20 h. (3) The acid-treated CNF was heated in a nitrogen atmosphere for 120 min at 200, 300, 350, and 450 °C, giving the CNF samples with various concentration of carboxylic species, which were designated as CNF200, CNF300, CNF350, and CNF450, respectively.

2.2 CNF-Supported Ru Catalysts

CNF-supported Ru catalysts were prepared by incipient wetness impregnation method using $RuCl_3 \cdot xH_2O$ as metal precursors. The impregnated samples were aged in air at room temperature for 20 h, then dried at 110 °C for 20 h, and calcined at 200 °C for 4 h in air. For comparison purpose, γ-Al_2O_3-supported Ru catalyst was prepared with the same method. Furthermore, γ-Al_2O_3 and SiO_2-supported TPAP catalysts (TPAP/γ-Al_2O_3 and TPAP/SiO_2) were also prepared by incipient wetness impregnation with tetra-*n*-propylammonium perruthenate (TPAP) solution, followed by dryness at 120 °C. The Ru loading of all catalysts was 2.0 wt%.

The reduction of the CNF and γ-Al_2O_3-supported Ru catalysts was performed in a mixed gas of H_2–N_2 with 6% H_2 (40 mL/min, STP) from room temperature to 200 °C with a heating rate of 2 °C/min and holding at 200 °C for 100 min. Then, the catalyst was purged by N_2 (99.99%, 40 mL/min STP) at 190 °C for 100 min in order to eliminate chemisorbed hydrogen. After cooling down to room temperature in N_2 flow, the reduced sample was calcined in flowing oxygen (40 mL/min, STP) from room temperature to 200 °C with a heating rate of 1 °C/min and holding at 200 °C for 100 min. This sample was designated as Ru/CNF200. Furthermore, Ru/CNF200 was heated in a nitrogen flow for 100 min at 300, 350, and 450 °C for the removal of partical carboxylic species, and these samples were designated as Ru/CNF300, Ru/CNF350, and Ru/CNF450, respectively.

2.3 Characterization

Nitrogen physisorption of CNF samples was carried out using a Micromeritics ASAP 2010M system. The sample was degassed for 20 h at 200 °C before the measurement. The infrared spectra of CNF samples were recorded on a Bruker Vertex 70 FTIR spectrometer. Transmission electron micrograph (TEM) images of CNF-supported ruthenium catalysts were performed on a JEOL JSM-3010 instrument operating at 300 kV.

The numbers of acid sites of treated CNF samples were determined by performing standard acid-base titrations [40]. As a typical run, 30 mg of CNF sample was stirred with 25 mL of a solution containing 0.1 M of NaCl and 0.1 mM of oxalic acid in deionized water, acidified to pH = 3 with 0.1 M of HCl. While stirring, pure nitrogen was bubbled through the slurry and 0.01 M of NaOH solution was added dropwise from a buret until the end-point (pH = 7.5) had been reached. Also, a blank experiment was done with 25 mL of a solution containing 0.1 M NaCl and 0.1 mM oxalic acid in deionized water. The number of acid sites on CNF samples was estimated by the difference in volume added compared to the blank.

For temperature-programmed desorption (TPD), benzyl alcohol was firstly adsorbed on CNF-supported catalysts at 140 °C for 3 h under the pressure of nitrogen (50 atm) in 50 mL autoclave. After washing with ethanol and drying at 110 °C for 12 h, sample was treated in flowing N_2 gas (40 mL/min STP) from room temperature to 150 °C with a heating rate of 2 °C/min and holding temperature at 150 °C for 120 min. Then, the curves of benzyl alcohol TPD were recorded in the range of 150–700 °C with heating rate 8 °C/min.

2.4 Catalytic Tests

Oxidation of benzyl alcohol was carried out in batch mode in a 50 mL of autoclave equipped with a magnetic stirrer. The reaction conditions were typically as follows: 3 mL of benzyl alcohol (0.029 mol), 50 mg of the catalyst, reaction temperature at 140 °C, oxygen pressure of 5 MPa, and reaction time for 3 h. The reaction products were analyzed by a gas chromatograph (Agilent 6890N GC).

3 Results and Discussion

Figure 1 shows nitrogen isotherms of various CNF samples, giving very similar hysteresis loop at a relative pressure $0.8 < P/P_0 < 1.0$ (Fig. 1a). Correspondingly, these samples exhibited close pore sizes (near 5–30 nm, Fig. 1b) and BET surface areas (92–114 m^2/g, Table 1). These results suggest that there is almost no obvious change in textural parameters for CNF samples by the treatment in nitrogen flowing at 200–450 °C.

Figure 2 shows the infrared spectra of various CNF samples. The IR spectrum of CNF200 exhibited obvious bands at 1,735, 1,587, 1,400 cm^{-1} (Fig. 2a). The band at 1,735 cm^{-1} is attributed to the C=O stretching vibration of carboxylic groups; the band at 1,400 cm^{-1} is assigned to –OH vibration in carboxylic acid species [41–44]; the band at 1,587 cm^{-1} is related to carbon skeleton vibration of aromatic rings [43–45]. Interestingly, after heating at 300–450 °C in nitrogen flow, the intensities of 1,735 and 1,400 cm^{-1} band over CNF300, CNF350, and CNF450 samples were reduced remarkably, suggesting that the carboxylic species could be significantly removed [43]. Furthermore, the acid-base titration shows quantitative data for carboxylic species over these samples, as presented in

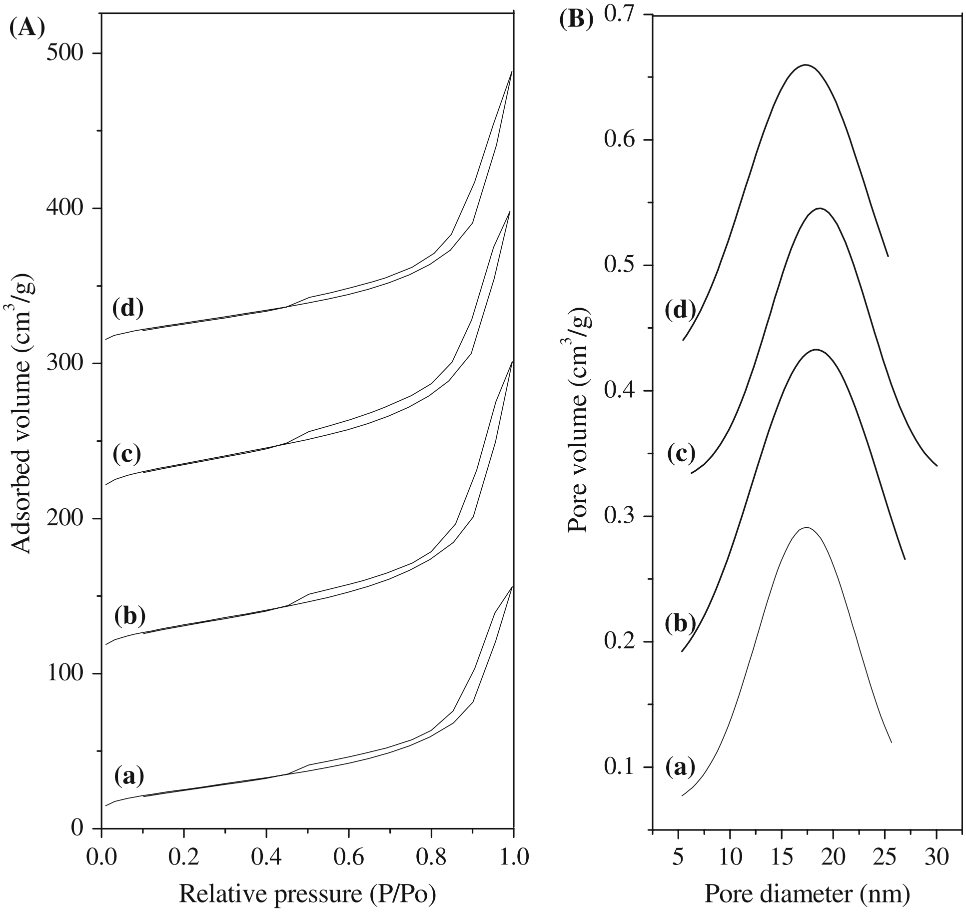

Fig. 1 **A** N_2 adsorption/desorption isotherms and **B** pore size distribution of (a) CNF200, (b) CNF300, (c) CNF350 and (d) CNF450. Isotherms of b, c and d have been offset by 100, 200, and 300 cm^3 g^{-1}, and the pore size distribution of b, c, and d have been offset by 0.1, 0.2, and 0.35 cm^3 g^{-1} along the vertical axis for clarity, respectively

Table 1 Textural parameters and acidic site density of CNF samples

Samples	BET surface area (m^2/g)	External surface area (m^2/g)	Mesoporous volume (cm^3/g)	Acidic site density (μmol/m^2)
CNF200	92	90	0.19	3.30
CNF300	114	111	0.23	1.96
CNF350	101	98	0.22	1.41
CNF450	94	94	0.22	0.73

Table 1. CNF200 has carbonxylic density of 3.30 μmol/m^2. When treated at 300 °C in nitrogen flow, CNF300 showed carbonxylic density at 1.96 μmol/m^2. After the treatment at 450 °C, CNF450 gave the value at 0.73 μmol/m^2 only. These results confirm that heating indeed results in the removal of partial carboxylic groups.

Figure 3 shows TEM images of various Ru/CNF samples. Notably, they exhibited similar particle sizes of ruthenium oxides (about 2–5 nm). The average particle sizes are about at 2.8, 3.0, 3.1, and 3.0 nm for Ru/CNF200, Ru/CNF300, Ru/CNF350, and Ru/CNF450, respectively. These results suggest that heating treatment at the temperatures of 200–450 °C in nitrogen flowing almost does not influence the particle distribution of ruthenium oxides.

Table 2 presents catalytic performances in oxidation of benzyl alcohol with molecular oxygen over various samples. CNF200 showed the conversion of benzyl alcohol at 16.4% (Run 1), which is a little more than a blank test (12.8%, Run 2). Notably, CNF-supported ruthenium catalysts have high catalytic activities. Particlularly, Ru/CNF200 catalyst gave very high activity at 70.9% (Run 4), which is comparative with that of TPAP/γ-Al_2O_3 (72.1%, Run 12) and TPAP/SiO_2 (68.6%, Run 13) [46, 47]. Interestingly, the sample activities remarkably decreased with increasing temperatures for the treatment of Ru/CNF200 catalyst. For example, after treatment at 450 °C in nitrogen flow, Ru/CNF450 showed the conversion at 30.4% (Run 8), which is even slightly less than Ru/Al_2O_3 (33.6%, Run 3). Generally, the catalytic performance of

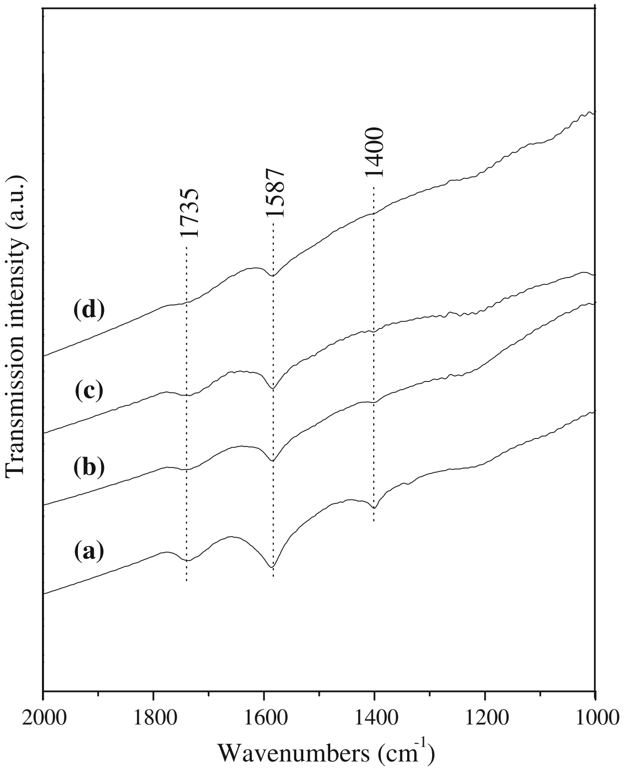

Fig. 2 Infrared spectra of **a** CNF200, **b** CNF300, **c** CNF350, and **d** CNF450 samples in the region of 2,000–1,000 cm^{-1}

supported metal catalysts was influenced by many parameters, such as metal dispersion, metal electronic state, and support properties. For a series of CNF-supported Ru catalysts in this work, Ru loading (about 2 wt%) is the same, Ru particle sizes are very similar, and the procedures for preparation of Ru particles are the same, only difference is their distinguishable number of carboxylic species. Therefore, it is proposed that carboxylic groups on the catalysts play an important role for the promotion of catalytic activity in oxidation of benzyl alcohol. To confirm this idea, a 10 mg of sodium benzoate was added into the reaction system, leading to higher activity (Run 8), the conversion of benzyl alcohol was increased up to 78.5% from 70.9% in the absence of sodium benzoate (Run 4).

To understand the role of carboxylic species, temperature-programmed desorption (TPD) of benzyl alcohol over Ru/CNF200 and Ru/CNF450 catalysts was carried out. As observed in Fig. 4, it is interesting to note that Ru/CNF450 has much larger amount of benzyl alcohol than Ru/CNF200, which should be reasonably assigned to their distinguishable carboxylic species. Recently, Toebes et al. [16] carefully compared the catalytic activities in cinnamaldehyde hydrogenation over Pt particles supported by CNF and carboxylic-functionalized CNF, and they suggested that the presence of carboxylic species on the

Fig. 3 TEM images of **a** Ru/CNF200, **b** Ru/CNF300, **c** Ru/CNF350, and **d** Ru/CNF450 catalysts

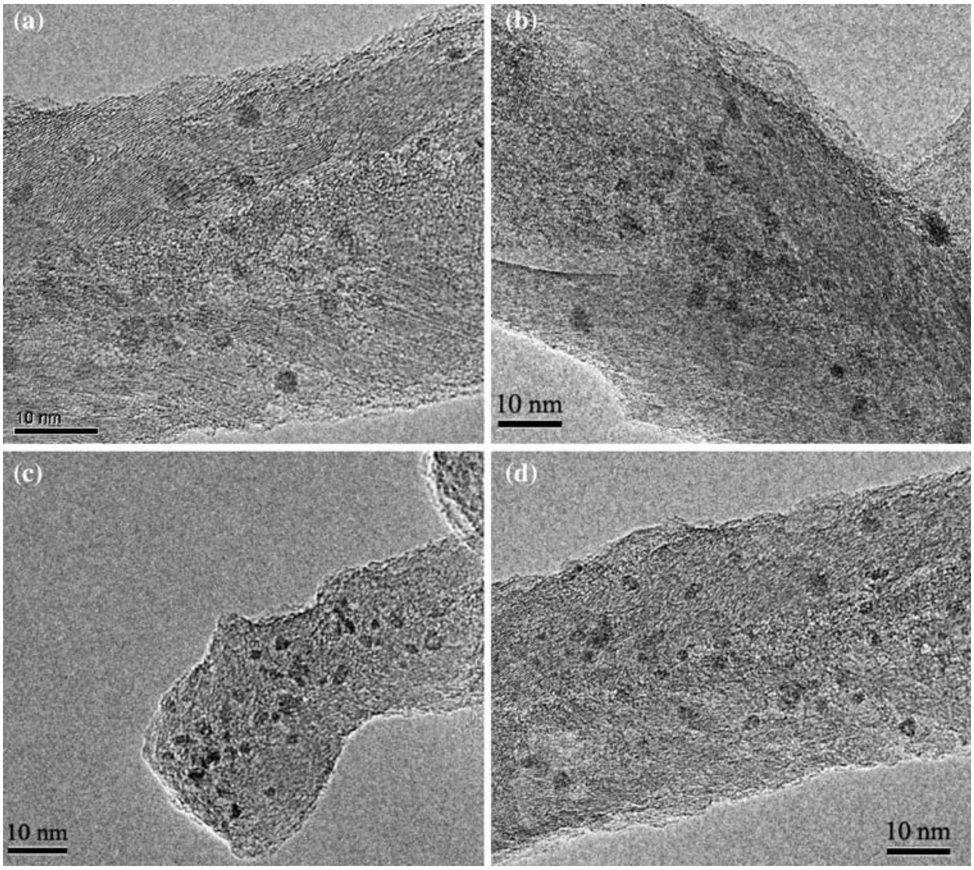

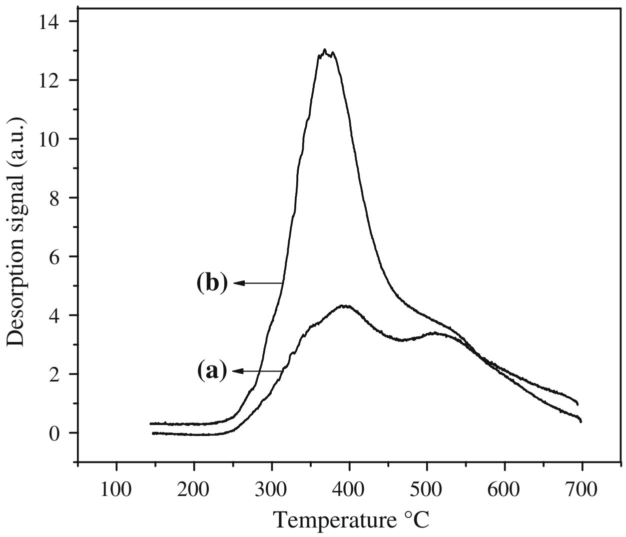

Fig. 4 TPD profiles of **a** Ru/CNF200 and **b** Ru/CNF450 after adsorption of benzyl alcohol on the catalyst, washing with ethanol at room temperature, and dryness at 120 °C

surface of CNF sterically hinders the adsorption of cinnamaldehyde by the π–π interaction between benzyl ring of cinnamaldehyde with non-polar CNF surface. Similarly, a large amount of carboxylic groups on the surface of Ru/CNF200 might sterically influence the adsorption of benzyl alcohol due to the difficulty of π–π interaction, compared with partially removed carboxylic species of Ru/CNF450. On the contrary, the difficulty of π–π interaction for the adsorption of benzyl alcohol on carboxylic-functionalized Ru/CNF200 might lead to relatively easy interaction of alcohol group in benzyl alcohol with carboxylic species due to hydrogen-bond effect [41, 42], therefore activating the alcohol group in the reactants. When this activated alcohol group was close to oxygen atom dissociated from ruthenium species in the case of Ru/CNF200 (Run 4 in Table 2), benzyl alcohol was easily converted into benzyl aldehyde. In contrast, if alcohol group was shortage of carboxylic species in the case of Ru/CNF450 (Run 7 in Table 2), the conversion of benzyl alcohol would require relatively high activation energy.

Furthermore, Ru/CNF300 catalyst was recycled for two times in order to study catalyst life, giving the conversion at 63.4 and 62.3% (Run 9 and 10 in Table 2), respectively. These results indicate that carboxylic-functionalized CNF-supported ruthenium catalysts are basically stable in oxidation of benzyl alcohol with molecular oxygen. Additionally, after removal of Ru/CNF300 in the reactor by a centrifugation for the first run (Run 5 in Table 2), a partial clear solution obtained was used to catalyze this oxidation again. By subtraction of the contribution in the first run, the net conversion for benzyl alcohol was 9.6% (Run 11 in Table 2), which is similar to that of blank run (Run 2 in Table 2). These results suggest that there is no leaching for the active sites over carboxylic-functionalized CNF-supported ruthenium catalysts.

Table 2 Catalytic properties in oxidation of benzyl alcohol with molecular oxygen over various samples

Run	Cataslysts	Conversion (%)	TOF (mol/g h)	Selectivity (%)		
				Benzaldehyde	Benzoic acid	Others
1	CNF200	16.4		98.6	1.4	
2	Blank	12.8		99.2	0.8	
3	Ru/Al_2O_3	33.6	3.2	98.6	1.4	
4	Ru/CNF200	70.9	6.9	83.8	14.7	1.5
5	Ru/CNF300	65.6	6.3	91.6	8.4	
6	Ru/CNF350	40.8	3.9	96.0	4.0	
7	Ru/CNF450	30.4	2.9	96.7	3.3	
8	Ru/CNF200[a]	78.5	7.6	80.1	18.1	1.8
9	Ru/CNF300[b]	63.4	6.1	91.0	9.0	
10	Ru/CNF300[c]	62.3	6.0	92.9	7.1	
11	Ru/CNF300[d]	9.6[e]	0.9	99.4	0.6	
12	TPAP/γ-Al_2O_3	72.1	7.0	79.8	17.5	2.7
13	TPAP/SiO_2	68.6	6.6	86.1	12.3	1.6

[a] 10 mg (0.0694 mmol) of sodium benzoate was added into reaction system

[b] Ru/CNF300 catalyst was recycled for first times

[c] Ru/CNF300 catalyst was recycled for second times

[d] After the removal of Ru/CNF300 catalyst in the reactor by a centrifugation for the first run (Run 5), a partial clear solution obtained was used to catalyze this oxidation again

[e] Net conversion by the subtraction of the contribution in the Run 5

4 Conclusion

Carboxylic-functionalized carbon nanofiber-supported ruthenium catalysts are catalytically active for oxidation of benzyl alcohol with molecular oxygen, and the partial removal of carboxylic species on the catalysts results in a significant reduction of catalytic conversion. Obviously, carboxylic species in these catalysts play an important role for improving catalytic property.

References

1. Serp P, Corrias M, Kalck P (2003) Appl Catal A 253:337
2. Rodriguez NM, Kim MS, Baker RTK (1994) J Phys Chem B 98:13108
3. Chambers A, Nemes T, Rodriguez NM, Baker RTK (1998) J Phys Chem B 102:2251
4. Park C, Baker RTK (1998) J Phys Chem B 102:5168
5. Park C, Baker RTK (1999) J Phys Chem B 103:2453
6. Giordano R, Serp P, Kalck P, Kihn Y, Schreiber J, Marhic C, Duvail JL (2003) Eur J Inorg Chem 610
7. Salman F, Park C, Baker RTK (1999) Catal Today 53:385
8. Planeix JM, Coustel N, Coq B, Brotons V, Kumbhar PS, Dutartre R, Geneste P, Bernier P, Ajayan PM (1994) J Am Chem Soc 116:7935
9. Pham-Huu C, Keller N, Charbonniere LJ, Ziessel R, Ledoux MJ (2000) Chem Commun 1871
10. Pham-Huu C, Keller N, Ehret G, Charbonniere JL, Ziessel R, Ledoux MJ (2001) J Mol Catal A 170:155
11. Ledoux MJ, Vieira R, Pham-Huu C, Keller N (2003) J Catal 216:333
12. Nhut JM, Vieira R, Pesant L, Tessonnier JP, Keller N, Ehret G, Pham-Huu C, Ledoux MJ (2002) Catal Today 76:11
13. Toebes ML, Prinsloo FF, Bitter JH, van Dillen AJ, de Jong KP (2003) J Catal 214:78
14. Brotons V, Coq B, Planeix JM (1997) J Mol Catal 116:397
15. Lordi V, Yao N, Wei J (2001) Chem Mater 13:733
16. Toebes ML, Nijhuis TA, Hájek J, Bitter JH, van Dillen AJ, Murzin DY, de Jong KP (2005) Chem Eng Sci 60:5682
17. Toebes ML, Zhang YH, Hájek J, Nijhuis TA, Bitter JH, van Dillen AJ, Murzin DY, Koningsberger DC, de Jong KP (2004) J Catal 226:215
18. Li Y, Lai GH, Zhou RX (2007) Appl Surf Sci 253:4978
19. Hoogenraad MS (1995) Growth and utilization of carbon fibrils. PhD thesis, The Netherlands, Utrecht University
20. Zhao Y, Li CH, Yu ZX, Yao KF, Ji SF, Liang J (2007) Mater Chem Phys 103:225
21. Li CH, Yu ZX, Yao KF, Ji SF, Liang J (2005) J Mol Catal A: Chem 226:101
22. Ros TG, Keller DE, Van Dillen AJ, Geus JW, Koningsberger DC (2002) J Catal 211:85
23. Gao R, Tan CD, Baker RTK (2001) Catal Today 65:19
24. Chen HB, Lin JD, Cai Y, Wang XY, Yi J, Wang J, Wei G, Lin YZ, Liao DW (2001) Appl Surf Sci 180:328
25. Liang CH, Li ZL, Qiu JH, Li C (2002) J Catal 211:278
26. Liu ZJ, Yuan ZY, Zhou WZ, Peng LM, Xu ZD (2001) Phys Chem Chem Phys 3:2518
27. Liu ZJ, Xu ZD, Yuan ZY, Lu DY, Chen WX, Zhou WZ (2001) Catal Lett 72:203
28. van Steen E, Prinsloo FF (2002) Catal Today 71:327
29. Bahome MC, Jewell LL, Hildebrandt D, Glasser D, Coville NJ (2005) App Catal A 287:60
30. Bezemer GL, Radstake PB, Falke U, Oosterbeek H, Kuipers HPCE, van Dillen AJ, de Jong KP (2006) J Catal 237:152
31. Bahome MC, Jewell LL, Padayachy K, Hildebrandt D, Glasser D, Datye AK, Coville NJ (2007) Appl Catal A 328:243
32. Luo JZ, Gao LZ, Leung YL, Au CT (2000) Catal Lett 66:91
33. Baker RTK, Laubernds K, Wootsch A, Paál Z (2000) J Catal 193:165
34. Wang MW, Li FY, Zhang RB (2004) Catal Today 93–95:603
35. Pawelec B, Parola VL, Navarro RM, Murcia-Mascarós S, Fierro JLG (2006) Carbon 44:84
36. Garcia J, Gomes HT, Serp P, Kalck P, Figueiredo JL, Faria JL (2005) Catal Today 102–103:101
37. Garcia J, Gomes HT, Serp P, Kalck P, Figueiredo JL, Faria JL (2006) Carbon 44:2384
38. Delgado JJ, Su DS, Rebmann G, Keller N, Gajovic A, Schlögl R (2006) J Catal 244:126
39. Piao LY, Li YD, Chen JL, Chang L, Lin JYS (2002) Catal Today 74:145
40. Toebes ML, van Heeswijk JMP, Bitter JH, van Dillen AJ, de Jong KP (2004) Carbon 42:307
41. Shaffer MSP, Fan X, Windle AH (1998) Carbon 36:1603
42. Chen J, Hamon MA, Hu H, Chen Y, Rao AM, Eklund PC, Haddon RC (1998) Science 282:95
43. Ros TG, van Dillen AJ, Geus JW, Koningsberger DC (2002) Chem Eur J 8:1151
44. Martínez MT, Callejas MA, Benito AM, Cochet M, Seeger T, Ansón A, Schreiber J, Gordon C, Marhic C, Chauvet O, Fierro JLG, Maser WK (2003) Carbon 41:2247
45. Mawhinney DB, Naumenko V, Kuznetsova A, Yates JT (2000) J Am Chem Soc 122:2383
46. Bleloch A, Johnson BFG, Ley SV, Price AJ, Shephard DS, Thomas AW (1999) Chem Commun 1907
47. Ciriminna R, Campestrini S, Pagliaro M (2004) Adv Synth Catal 346:231